Vibrational relaxation in clusters: Energy transfer in $I_2^-(CO_2)_4$ excited by femtosecond stimulated emission pumping

Alison V. Davis, Roland Wester, Arthur E. Bragg, and Daniel M. Neumark
Department of Chemistry, University of California, Berkeley, California 94720 and Chemical Sciences Division, Lawrence Berkeley National Laboratory, Berkeley, California 94720

(Received 18 April 2002; accepted 7 June 2002)

Vibrational relaxation dynamics in $I_2^-(CO_2)_4$ clusters are monitored by femtosecond stimulated emission pumping in conjunction with femtosecond photoelectron spectroscopy. Femtosecond pump and tunable dump pulses coherently excite the I_2^- within the cluster with vibrational energies ranging from 0.57 to 0.86 eV; the subsequent dynamics are monitored via the time-dependent photoelectron spectrum, and are compared to those resulting from excitation of bare I_2^-. Two observables are used to follow the vibrational relaxation from the vibrationally excited I_2^- to the surrounding solvent molecules. From 0 to 4 ps, relaxation is apparent through a time-dependent increase in the oscillation which is monitored at its inner turning point. At longer times, out to ~100 ps, shifts in the photoelectron spectra are used to determine the vibrational energy content of the I_2^-. Indirect evidence is presented for early rapid energy loss during the first half-oscillation of the wave packet across the potential. © *2002 American Institute of Physics.* [DOI: 10.1063/1.1497160]

I. INTRODUCTION

The relaxation dynamics of highly vibrationally excited molecules is a subject that extends across many areas of chemical physics, with innumerable experimental and theoretical investigations having been carried out in gas and condensed phases. One of the main thrusts of gas phase research, as reviewed by Flynn *et al.*,[1] has been the understanding of state-to-state energy transfer between vibrationally excited small molecules such as I_2, O_2, and NO, and collision partners which are often either rare gases or other small molecules. Sophisticated preparation methods such as stimulated emission pumping (SEP) (Ref. 2) have been used to prepare completely characterized reactants, and vibrational energy transfer in individual collisions has been widely studied. Vibrational relaxation of highly excited chromophores in solution, reviewed by Stratt and Maroncelli,[3] has been extensively studied by time-dependent methods, with collective solvent modes implicated in much of the fast relaxation observed in polar solvents.

Clusters provide an intermediate size environment in which to study vibrational energy relaxation and redistribution, allowing one to understand how the binary collision dynamics in gas phase experiments evolve into the more collective dynamics in condensed phases. Anion clusters of the form $I_2^-(S)_n$, where S is a solvent species, have proved to be a particularly useful model system for studying vibrational relaxation,[4–11] in part because the charged clusters can be readily size-selected, and also because comparison can be made with numerous condensed phase studies of I_2^- dynamics in polar solvents.[12–22] In these studies, vibrationally excited I_2^- in its ground electronic state is produced either after dissociation and solvent-induced caging (in both the cluster and solution-phase experiments)[4,8,12] or as a product of the dissociation of I_3^- (in polar solvents).[18,21]

Ground state coherences and vibrational relaxation are evident in some these studies, but dynamics due to the upper-state processes of dissociation and recombination can be difficult to separate from those of interest on the ground state. For example, in time-resolved photoelectron spectroscopy studies in our laboratory,[9,11] significant recombination and vibrational energy loss were observed after dissociating $I_2^-(CO_2)_n (6 \leqslant n \leqslant 16)$ clusters, but because ~0.56 eV excess energy had to be dissipated in order for ground state recombination to occur (the difference between the photon energy and the I_2^- bond dissociation energy), energy transfer to the solvent network was well underway before vibrational relaxation of the newly-recombined chromophore could begin. Hence recombination, vibrational energy loss, and evaporation could not be completely deconvoluted, complicating the interpretation of the spectra.

In the experiment described here, this problem is circumvented experimentally by coherently exciting the I_2^- chromophore in $I_2^-(CO_2)_4$ with a well-defined vibrational energy using femtosecond stimulated emission pumping (SEP). In most SEP experiments, pump and dump pulses from a cw or nanosecond laser are used to populate high vibrational eigenstates, enabling the study of their spectroscopy and their relaxation dynamics and reactivity in collisions with other molecules.[2] Femtosecond SEP, in which both the pump and the dump pulses are short in time with high bandwidth, produces nonstationary wave packets comprised of several vibrational eigenstates.[23–27] In our laboratory, we probe the evolving wave packet with femtosecond photoelectron spectroscopy (FPES).[25,28,29] Other groups have used three-photon ionization[23] or time-resolved four-wave mixing spectroscopy[26,27] as a probe. Most femtosecond SEP work to date has involved diatomic molecules; in its first application in our group, we examined I_2^- at several ground-state excitation energies, up to 90% of the dissociation limit, and used the energy-dependent wave packet oscillation fre-

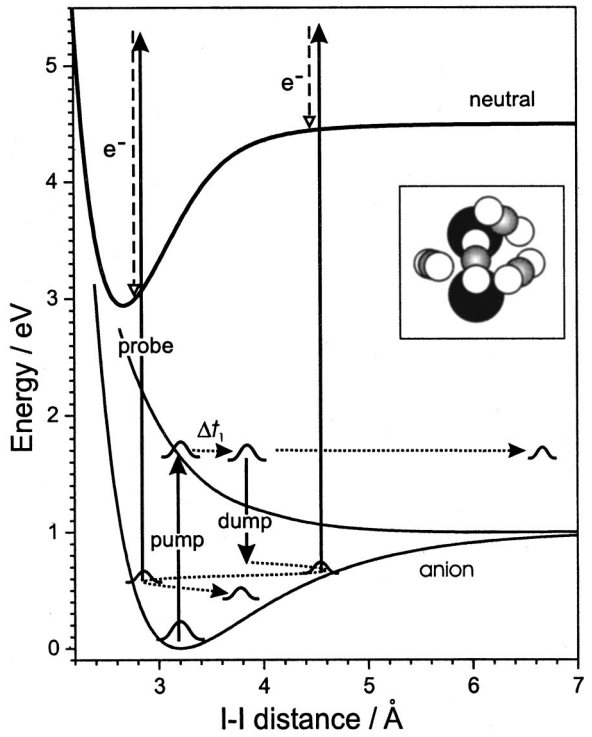

FIG. 1. Schematic of SEP-FPES experiment for $I_2^-(CO_2)_4$. Potential energy curves (bottom to top) are for $X\,^2\Sigma_u^+$ and $A'\,^2\Pi_{g,1/2}$ states of I_2^- and $X\,^1\Sigma_g^+$ state of I_2, with appropriate solvent shift of anion vs neutral curves for $n=4$ cluster. The inset shows the calculated structure for $I_2^-(CO_2)_4$ (Ref. 49).

quencies and revival times to characterize the ground state potential.[25]

Our implementation of SEP-FPES is illustrated in Fig. 1. An ultrafast pump pulse promotes the I_2^- moiety within $I_2^-(CO_2)_4$ to the dissociative $\tilde{A}'\,^2\Pi_{g,1/2}$ state, after which a tunable ultrafast dump pulse stimulates a portion of the excited state wave packet back to the $\tilde{X}\,^2\Sigma_u^+$ state. The result is a vibrationally excited wavepacket with energy $E_{\rm exc}$ given by

$$E_{\rm exc}=h\nu_{\rm pump}-h\nu_{\rm dump}. \tag{1}$$

A femtosecond UV pulse (the probe pulse) detaches the electron at a second delay, and by stepping the probe timing, time-dependent PE spectra are obtained. In bare I_2^-, the wave packet oscillates without losing energy, dephasing and rephasing indefinitely as the wavepacket delocalizes and subsequently revives. In a cluster, the energy initially located in the I–I stretch eventually dissipates into the various solvent modes, and the initially formed ''SEP wave packet'' should move down in the well, as shown qualitatively in Fig. 1. In either case, using FPES as the probe allows one to follow the wave packet dynamics in detail. It is most useful to study a small cluster such as $I_2^-(CO_2)_4$ that exhibits little solvent-induced caging from the excited state, so that the only vibrationally excited ground state intensity is due to the SEP wave packet.

We have previously reported preliminary SEP-FPES results for I_2^- in a cluster of four CO_2 molecules at a single excitation energy.[29] More recently, we used photofragment mass spectrometry to measure the extent of CO_2 evaporation from $I_2^-(CO_2)_4$ and $I_2^-(CO_2)_5$ as a function of $E_{\rm exc}$, thereby determining the binding energy of each solvent molecule to the cluster.[30] In the work discussed here, we present a complete study of the $n=4$ cluster where excitation energies between 0.57 eV and 0.86 eV—significant compared to the I_2^- dissociation energy[25] of 1.01 eV—are examined, and FPES is used to probe the dynamics on timescales ranging from femtoseconds to hundreds of picoseconds.

The FPE spectra are particularly sensitive to the wavepacket dynamics at its inner turning point (ITP). Two observables are used to follow the vibrational relaxation from the vibrationally excited I_2^- to the surrounding solvent molecules. Oscillations associated with ITP dynamics are observed at dump-probe delays of 0–4 ps, and vibrational relaxation is apparent through a time-dependent increase in the frequency of these oscillations. At times out to ~100 ps, shifts in the PE spectra are used to determine the vibrational energy content of the I_2^-. These two sets of measurements yield a detailed picture of vibrational relaxation dynamics in $I_2^-(CO_2)_4$.

II. EXPERIMENT

The anion source and femtosecond laser system have been described elsewhere;[9,31] only a brief overview is given here. A mixture of 2.5% CO_2 in Ar carrier gas is passed at 20 psi over solid I_2 and through a piezoelectric pulsed valve operating at a repetition rate of 500 Hz. The resulting supersonic expansion is crossed by a 1.2 keV beam from an electron gun, creating ions and clusters. The beam passes through a skimmer and enters a differential chamber, where the anions are extracted in a Wiley–McLaren mass spectrometer. After passing through two additional differential regions, mass-selected clusters are intersected by the pump, dump, and probe laser pulses. The ejected electrons are collected with >50% efficiency in a magnetic bottle time-of-flight analyzer.

A Clark-MXR amplified Ti:sapphire laser system produces 90 fs pulses at 790 nm (1.57 eV), at energies of 1 mJ/pulse and a repetition rate of 500 Hz. 60 μJ of this fundamental is used as the pump pulse, and 500 μJ is used to pump an optical parametric generator/amplifier (TOPAS; Light Conversion) to produce the tunable dump pulse (110 fs), which ranges in energy from 30 to 60 μJ/pulse and in wavelength from 1250 to 1520 nm (corresponding to $E_{\rm exc}$ from 0.57 to 0.86 eV). The remainder is used in a frequency-tripling unit to produce the 263 nm probe pulse (4.71 eV, 20 μJ/pulse, 130 fs). The pump and probe lasers pass through computer-controlled delay stages to allow independent optimization of the pump-dump timing and stepping of the dump-probe timing. The spectra of the pump and dump pulses were measured using either a monochromator or a fiberoptic spectrometer (Ocean Optics S2000).

For all but the highest excitation discussed here, the dump pulse was chopped (New Focus 3501) at half the laser repetition rate. The two-color spectra were dynamically subtracted from the three-color spectra on a shot-to-shot basis with a multichannel scaler (SRS SR430), and the two-color spectra were additionally collected and saved for normalization in a digital oscilloscope (Tektronix 744A). Typical col-

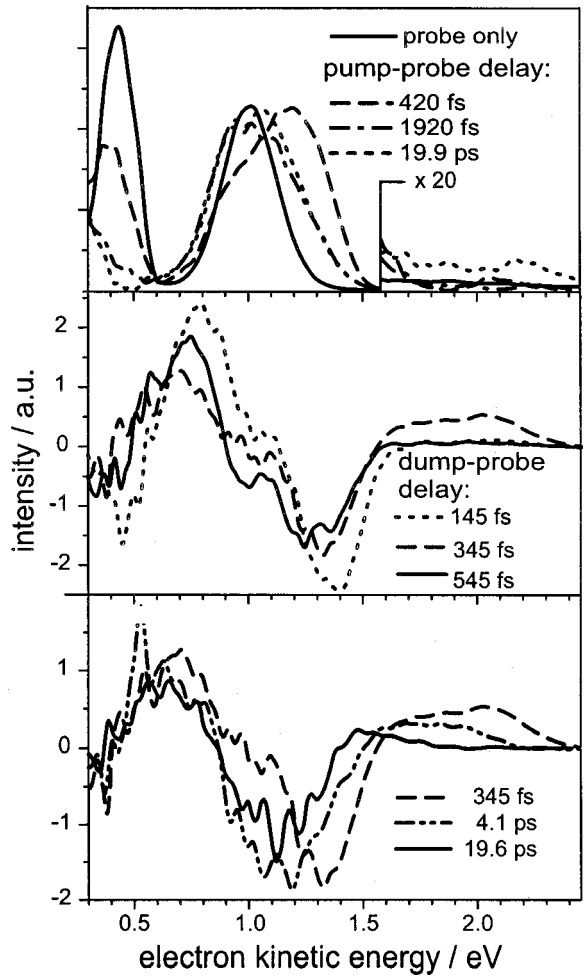

FIG. 2. (Top panel) Probe-only and pump-probe (no dump) spectra of $I_2^-(CO_2)_4$. A scaled amount of probe-only intensity has been subtracted from each pump–probe spectrum to highlight the excited-state dynamics. (Lower panels) Spectra of $I_2^-(CO_2)_4$ at $E_{exc}=0.57$ eV SEP. The pump-dump delay is 80 fs. Short dump-probe delays, middle panel, demonstrate initial intensity oscillations, while at long delays, bottom, the shift of the high-eKE edge to lower energies is apparent.

lection times were 50 s per spectrum. The zero-of-times inside the machine were determined by above-threshold-detachment of I^- by the pump and probe or dump and probe pulses. The optimum pump-dump delay for maximum SEP efficiency varied from 80 fs at $E_{exc}=0.57$ eV to 190 fs at 0.75 eV.

III. RESULTS

Figure 2 shows several PE spectra obtained with various combinations of pump, dump, and probe pulses. The *x*-axis shows the electron kinetic energy (eKE). The solid line in the top panel shows the ''probe-only'' spectrum, i.e., the PE spectrum of $I_2^-(CO_2)_4$ at 263 nm, recently reported by us at considerably higher resolution.[32] The peak at eKE=1.1 eV is due to detachment from the cluster anion ground state to the neutral $\tilde{X}$ state, while the peak at 0.5 eV is from unresolved detachment to the $\tilde{A}$ and $\tilde{A}'$ states of I_2. The broken lines in the top panel show several pump–probe spectra for which a scaled amount of the probe-only spectrum has been subtracted, so that features due only to the combination of pump and probe pulses remain. The spectrum at 420 fs pump–probe delay shows the growth of a higher-energy peak extending to 1.5 eV. By 1920 fs the spectrum has shifted to lower eKE, and changes relatively little thereafter. However, a very small feature above 2 eV appears around 3 ps (not shown) and is shown nearly at its full extent in the 19.9 ps spectrum. As discussed previously,[11] the pump–probe spectra represent dynamics in the electronically excited cluster which, for this small cluster, are dominated by dissociation of the I_2^- chromophore on the repulsive $\tilde{A}'$ state. The feature above 2 eV is due to a small amount of vibrationally excited I_2^- produced by solvent-induced recombination.

The lower two panels in Fig. 2 show photoelectron spectra of $I_2^-(CO_2)_4$ obtained with the pump-dump-probe configuration at several dump-probe delays, with the dump pulse chosen so that $E_{exc}=0.57$ eV. These are difference spectra, i.e. (pump+dump+probe)−(pump+probe), with a pump-dump delay of 80 fs. In these spectra, features induced by the dump pulse have positive intensity, while those with negative intensity are associated with $\tilde{A}'$ state dynamics and result from the depletion of the excited $\tilde{A}'$ state wave packet by the dump pulse. The middle panel of Fig. 2 shows spectra at short dump-probe delay times. At 145 fs after the dump pulse, most of the positive intensity is concentrated around 0.8 eV. At 345 fs, the intensity around 0.8 eV has decreased significantly, and strong intensity has grown in at eKE >1.5 eV. By 545 fs, the intensity at high eKE is near zero, and the intensity around 0.8 eV is again at a maximum. It is clear that these spectra show oscillations as a function of dump-probe delay, and that the oscillations at eKE>1.5 eV and eKE≈ 0.8 eV are out of phase.

At times longer than ~4 ps, no oscillations are apparent in any region of the spectra. Instead, the high eKE edge of the spectrum shifts to lower kinetic energy, as shown in the bottom panel of Fig. 2. This shift is basically complete by 20 ps. As the shift occurs, it is apparent that the negative signal around 1.1 eV is being ''filled in'' by the dump pulse; although signal in this energy region does not change much after 2 ps in the pump–probe spectra, it becomes progressively less negative between 4 and 20 ps in the 3-photon spectra.

The oscillatory structure in the pump-dump-probe spectra can be followed by integrating the signal at high eKE (≈ 2.3 eV) and plotting the integral intensity as a function of time. The results for $I_2^-(CO_2)_4$ at four excitation energies are shown in Fig. 3, along with analogous results for bare I_2^- at the same excitation energies; all plots are scaled to have the same maximum height. Several trends are evident in Fig. 3. The oscillations dephase by 3–4 ps in $I_2^-(CO_2)_4$ compared to 7–9 ps in bare I_2^-.[25] While the frequency of the oscillations decreases with E_{exc} in bare I_2^-, this trend is not at all evident in $I_2^-(CO_2)_4$. At $E_{exc}=0.75$ eV and 0.86 eV, there is an increasingly nonoscillatory component to the integrated high energy signal for $I_2^-(CO_2)_4$. While the I_2^- oscillations reappear after about 45 ps due to the revival of the anion wave packet,[25] no revival is seen for $I_2^-(CO_2)_4$. Finally, in what is the least obvious trend by inspection but perhaps the most important, the oscillation frequency in the $I_2^-(CO_2)_4$

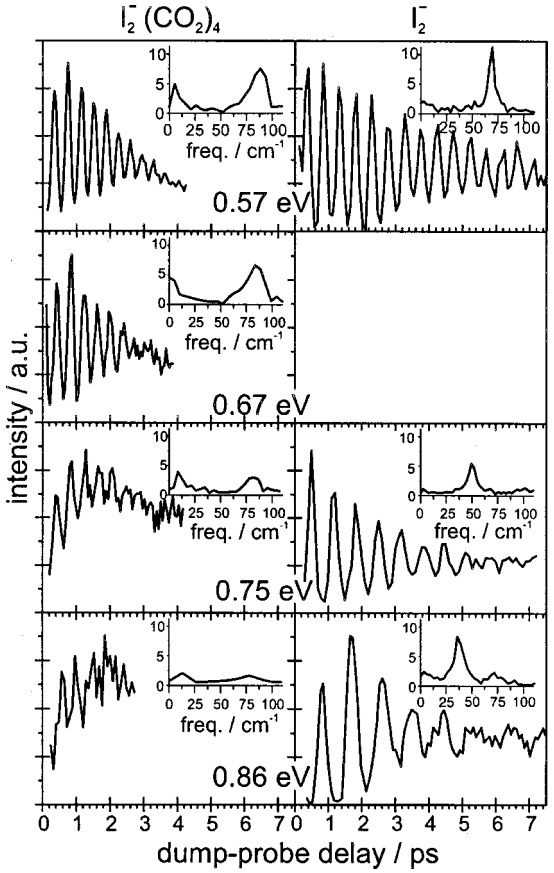

FIG. 3. Integrated high eKE signal for $I_2^-(CO_2)_4$ (left column) and I_2^- (right column) at four SEP excitation energies. Fourier transforms of each oscillation are shown in insets.

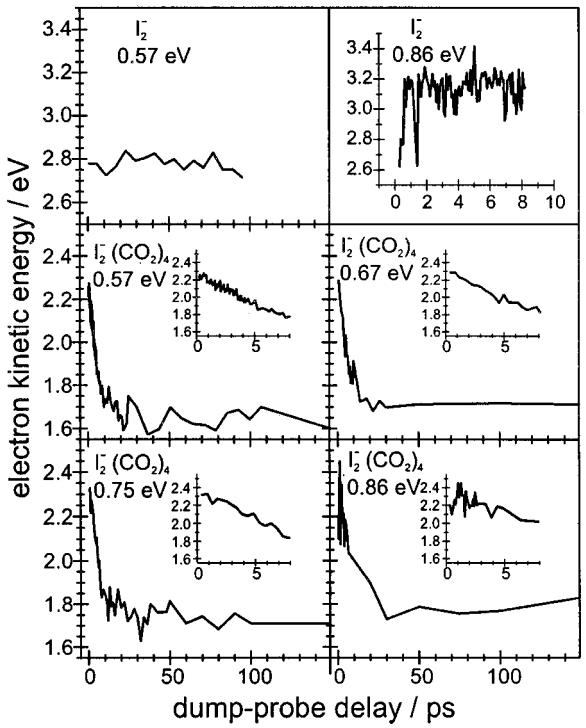

FIG. 4. Position of the high-eKE edge of the spectrum as function of dump-probe delay time. The top row shows data for bare I_2^- with 0.57 and 0.86 eV excitation energy; only a short time scale is shown for the latter. The bottom two rows display data for the cluster at four excitation energies; inset in each panel is an enlargement of the 0–8 ps time scale.

signals increases with time at each E_{exc}, whereas that for bare I_2^- remains constant.

The other clear time-dependent trend in Fig. 2 is the shift of the high eKE edge of the spectra toward lower energy. In Fig. 4, the position of this edge ("edge" being the energy at the half-height of the intensity of the highest energy signal in the pump-dump-probe spectra) is plotted for dump-probe delay times up to 150 ps for bare I_2^- at excitation energies of 0.57 and 0.86 eV, and at each of the four energies in Fig. 3 for $I_2^-(CO_2)_4$. The inset for each cluster energy shows a close-up of the first 8 ps. For bare I_2^- at 0.57 eV excitation, the edge of the spectrum is more or less constant in energy, around eKE$=2.8$ eV. When bare I_2^- is excited with 0.86 eV (upper right panel), the edge position remains constant near 3.2 eV except for two brief oscillations that coincide in time with the intensity variations at high eKE (Fig. 3). In the cluster, in contrast, excitation below 0.86 eV results in spectra where the edge energy quickly decreases, levels off by about 20 ps, and remains constant at the lower energy for hundreds of picoseconds. At 0.86 eV, where the high eKE signal is very low, there is a brief rise in energy around 1 ps, after which the edge decreases in energy with a time scale similar to the other excitations.

IV. ANALYSIS

The significance of the time-dependent trends at high eKE can be seen with reference to Fig. 1. Although the anion wave packet generated by SEP can be photodetached at any phase of its motion by the probe pulse, the energy difference between the anion and neutral ground states is smallest at its inner turning point (ITP), so photodetachment at the ITP will result in the highest energy photoelectrons. Closer examination of the curves in Fig. 1 shows that any electrons with eKE$\geqslant 1.5$ eV must come from near the ITP of vibrationally excited I_2^-. Hence, the high energy photoelectron signal considered in Figs. 3 and 4 reflects dynamics at the ITP. The dynamics induced by the dump pulse are evident at other electron energies as well. For example, the signal at eKE ≈ 0.8 eV in the middle panel of Fig. 2 is out-of-phase with the high energy signal and therefore reflects dynamics at the outer turning point of the wavepacket. However, in general, the signal in this energy range has contributions from dump-induced depletion and enhancement as well as transitions to multiple neutral electronic states, and its interpretation is considerably more complicated. In this section, we therefore focus on analysis of the high energy signal, considering both the oscillation in Fig. 3 and the energy shifts in Fig. 4, both of which are cleanly associated with ITP dynamics.

A. Oscillations at the inner turning point

The first step in analyzing the oscillations in Fig. 3 is to determine their Fourier transforms (FT's). These are shown in the insets in Fig. 3; the oscillations were shifted downward to be approximately centered on zero before Fourier transformation to reduce the zero-frequency component. The oscillation frequency reflects the energy separation between adjacent energy levels. For bare I_2^-, the frequency drops with

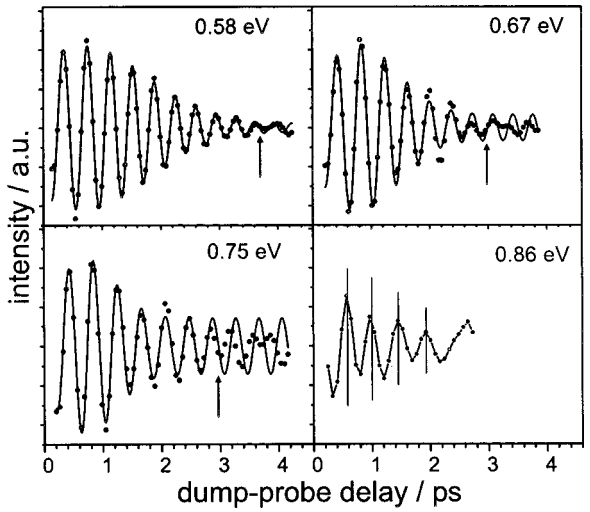

FIG. 5. Fits (smooth line) to smoothed inner turning point oscillations in $I_2^-(CO_2)_4$ (points) using Eq. (2) in text. For $E_{exc}=0.86$ eV, the oscillations were not fit; instead, the center of each maximum was determined individually. The fit parameters are given in Table I.

increasing excitation energy, from 69 cm^{-1} at $E_{exc}=0.57$ eV to 36 cm^{-1} at 0.86 eV, due to the anharmonicity of the I_2^- potential as discussed previously.[25] The FT's for the cluster are quite different. The center frequencies are considerably higher than for bare I_2^- at the same E_{exc}, e.g., 89 vs 69 cm^{-1} at 0.57 eV, and the cluster center frequencies do not drop appreciably with increasing E_{exc}.

A closer inspection of the cluster oscillations shows that their frequency increases with time; this effect contributes to the increased width of the cluster FT's compared to those of bare I_2^-. In order to probe this effect more quantitatively, each oscillation was fitted by a modified sinusoidal with a frequency linearly dependent on time. The results are shown in Fig. 5. Before fitting, the oscillations were shifted to be centered about zero and a FFT filter passing bandwidth between 0.5 and 1.5 times the peak in the overall FT was applied. Thus smoothed, the oscillation at each of the three lowest energies was fitted by a nonlinear least squares method with a function proportional to

$$\left[\exp\left(\frac{-(t-t_0)^2}{2w^2}\right)+y_0\right]\sin\left(2\pi t\left(f_0+\frac{a}{2}t\right)+\phi\right). \qquad (2)$$

The time-dependent, instantaneous frequency is determined by the derivative of the argument, f_0+at. The addition of a quadratically varying frequency component did not yield significantly better fits. The envelope is an offset Gaussian function, needed to account for the fact that the amplitude peaks at the second oscillation and does not decay to zero. The oscillations of bare I_2^- were fitted analogously, and it was confirmed that in the bare ion the frequency does not change significantly with time.

In Fig. 5, the data are shown as points, and the sinusoidal fits as smooth curves. Each arrow shows the extent of the data that was fitted, generally the last obvious oscillation. The oscillation at 0.57 eV was fitted between 195 and 3695 fs (10 oscillations), that at 0.67 eV was fitted between 263 and 2963 fs (7 oscillations), and the oscillation at 0.75 eV was fitted between 264 and 2964 fs (7 oscillations). The weak oscillations at 0.86 eV were not fit with a sine wave since there are only four maxima; instead, the oscillations were smoothed as above and then the center of each maximum (shown on Fig. 5 as vertical lines through the oscillations) was determined by fitting it to a Gaussian. The results of the frequency fits are given in Table I, and are shown as solid lines in Fig. 6. The linear frequency fit to the 0.75 eV oscillation has a much smaller slope than the fit to either of the lower energy excitations, and for all of these fits the slope of the frequency is positive. The three frequencies determined for $E_{exc}=0.86$ eV are shown as squares. The dashed lines in Fig. 6 show the (constant) frequencies for bare I_2^- derived from our previously determined I_2^- potential[25] at the same four excitation energies. At each E_{exc}, the extrapolated $t=0$ frequencies for the cluster are significantly higher than those for bare I_2^-, a point discussed in more detail in Sec. V.

TABLE I. Selected parameters from fits to smoothed oscillations in Fig. 5. See Eq. (2) in text.

E_{exc} (eV)	f_0 (cm^{-1})	a (cm^{-1}/ps)	t_0 (ps)	w (ps)
0.57	78.56±0.34	6.74±0.25	0.69±0.05	1.08±0.07
0.67	76.5±0.9	6.26±0.68	0.80±0.05	0.66±0.06
0.75	79.4±1.0	1.4±0.7	0.72±0.06	0.49±0.07

The increase in the oscillation frequencies with time provides a sensitive and direct probe of the vibrational relaxation dynamics in the clustered I_2^-; as the wave packet loses energy, the energy between adjacent I_2^- vibrational levels increases due to the anharmonicity of the potential. The time-dependent frequencies found for the cluster can be converted to time-dependent vibrational energies $E_{vib}(t)$ using the potential for bare I_2^-.[25] These energies are shown in Fig. 7, superimposed on energies derived from the edge shifts discussed below. In the case of the two lower excitations, $E_{vib}(t)$ decreases sharply over the period where oscillations are observed, e.g., 0.35 eV over 4 ps at $E_{exc}=0.57$ eV, while

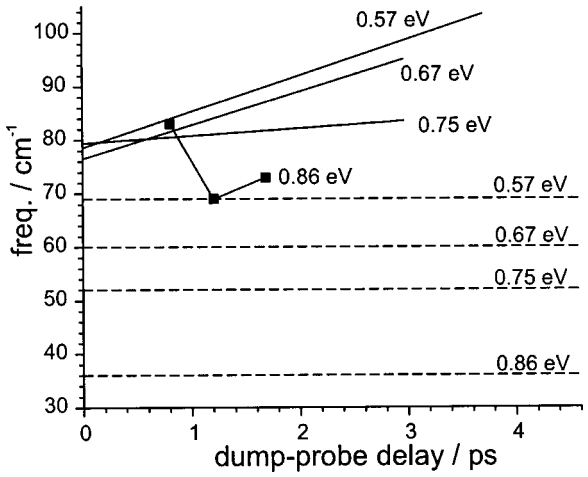

FIG. 6. Time dependent oscillation frequencies f_0+at (see Table I) for $I_2^-(CO_2)_4$ (solid lines) at $E_{exc}=0.57$, 0.67, and 0.75 eV. For the cluster at $E_{exc}=0.86$ eV, points connected by lines correspond to the three spacings between the first four maxima. Frequencies for bare I_2^- at the four excitation energies are shown as dashed lines (top, 0.57 eV; bottom, 0.86 eV).

the cluster excited with 0.75 eV exhibits only small losses in energy over 3 ps. From these energy losses, one can determine the number of vibrational quanta lost per oscillation Δv_{osc}. At $E_{exc}=0.57$ eV, Δv_{osc} drops from 3.7 for the first full oscillation (ITP to ITP), to 3.0 for the last (9th). For $E_{exc}=0.67$ eV, Δv_{osc} is 3.5 for the first oscillation and drops to 3 for the last (6th). For $E_{exc}=0.75$ eV, where rate of frequency change is much smaller, only about 4.6 quanta total are dissipated during the six round trips between 425 and 2875 fs.

B. Shift of the spectrum

The shift of the high kinetic energy edge of the PE spectra, as shown in Fig. 4, can also be used to follow the I_2^- vibrational relaxation dynamics in $I_2^-(CO_2)_4$, and has the advantage that it can be used at dump-probe delays times long after the oscillations have irreversibly decayed. The edge position is given by $h\nu_{probe}-VDE_{ITP}$, where $h\nu_{probe}$ is the photon energy of the probe pulse and VDE_{ITP} is the vertical detachment energy at the inner turning point of the I_2^- in whatever vibrational state it is in at the time. With reference to Fig. 1, it is clear that VDE_{ITP} increases as the I_2^- relaxes, resulting in a shift of the edge toward lower electron kinetic energy.

In order to convert the time-dependent edge positions to time-dependent I_2^- vibrational energies $E_{vib}(t)$, we assume the potentials for the anion and neutral clusters are the same as the potentials for the ground states of I_2^- and I_2,[25,33–35] but are shifted in energy relative to one another because the solvent molecules bind more strongly to the I_2^- than to the I_2. These "solvent shifts" are known from our photoelectron spectra of $I_2^-(CO_2)_n$ clusters;[32] the total shifts are 139, 250, 345, and 425 meV for $n=1-4$. The resulting values of $E_{vib}(t)$ are shown as the jagged lines in Fig. 7 for relatively short times (0–8 ps), and in Fig. 8 for longer times (0–100 ps).

Since evaporation of the solvent molecules may occur over the time scale of the experiment, vibrational energies in each panel were calculated for several cluster sizes with $n \leqslant 4$. Removal of a solvent molecule brings the anion and neutral potentials closer together; as a result, for a given edge position, the calculated E_{vib} is lower for a smaller cluster. Thus, in Figs. 7 and 8, the top curve is calculated for the $n=4$ cluster, the curve below for $n=3$, etc. The minimum number of CO_2 molecules for which E_{vib} was calculated is determined by the smallest significant product found in the daughter ion distribution at the excitation energy in question.[30]

At each excitation energy, the $n=4$ curve was fit to a single exponential decay curve of the form,

$$E_{vib}(t)=E_0+Ae^{-t/\tau}. \tag{3}$$

The best fit is shown as a dashed line at each excitation energy in Figs. 7 and 8, and the fitted parameters E_0, A, and τ are given in Table II. The fit for $E_{exc}=0.86$ eV was begun at 1 ps delay, coinciding with the maximum in energy. We find that τ, the time constant for vibrational relaxation, is in the range of 5 ps independent of excitation energy. At long

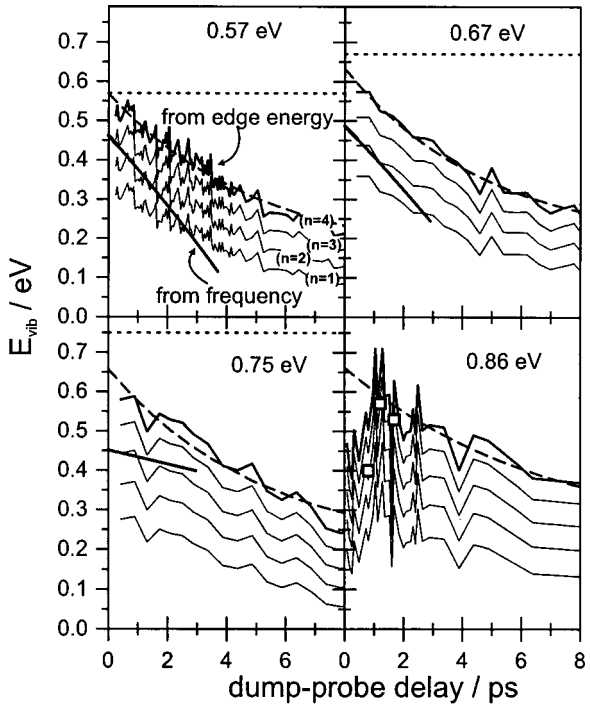

FIG. 7. Vibrational energy (E_{vib}) remaining for the cluster at early dump-probe delay times. Jagged lines are derived from the shift of the spectrum edge in Fig. 4, with the uppermost assuming 4 CO_2 molecules remaining, the one below assuming 3, etc. The smooth dashed curve through the $n=4$ curves in each panel represents an exponential fit using Eq. (3); parameters are given in Table II. For the cluster excited with 0.86 eV, the fit begins after the initial rise. The straight solid lines at 0.57, 0.67, and 0.75 eV are derived from the time-dependent frequency of the oscillations using the potential for bare I_2^-; the equivalent energies derived from frequencies for $E_{exc}=0.86$ eV are shown as small squares. For the lowest three excitation energies, $E_{exc}=h\nu_{pump}-h\nu_{dump}$ is shown as a horizontal dashed line.

times, E_{vib} does not decay to zero but to a residual energy E_0 that increases from 0.15 to 0.23 eV as the excitation energy is raised from 0.57 to 0.86 eV.

The accuracy of our procedure for determining E_{vib} can be gauged by its results for bare I_2^-, for which the vibrational energy is known and constant. Values of $E_{vib}(t)$ derived from the edge of the spectrum, shown in the top panels of Fig. 8, are too high, on average, by about 60 meV at $E_{exc}=0.57$ eV, and by about 100 meV at 0.86 eV. These discrepancies occur in part because of the limited electron energy resolution of the magnetic bottle analyzer when used with a fast ion beam. The resolution for I_2^- is approximately 0.35 eV in the region of the high energy edge, and for the ~2 eV electrons from $I_2^-(CO_2)_4$ it is approximately 0.25 eV. We therefore expect the determination of E_{vib} from edge positions to overestimate its value, although the extent of this effect in the cluster spectra is hard to quantify. We also note that in Fig. 7, $E_{vib}(t)$ determined from the oscillation frequencies is lower by about 0.1 eV, on average, than that determined by the edge positions. Some of this discrepancy may result from our electron energy resolution; other possible contributing factors, such as solvent evaporation on the time scale of the oscillations and errors in our method of extracting $E_{vib}(t)$ from the oscillation frequencies, are discussed in Sec. V.

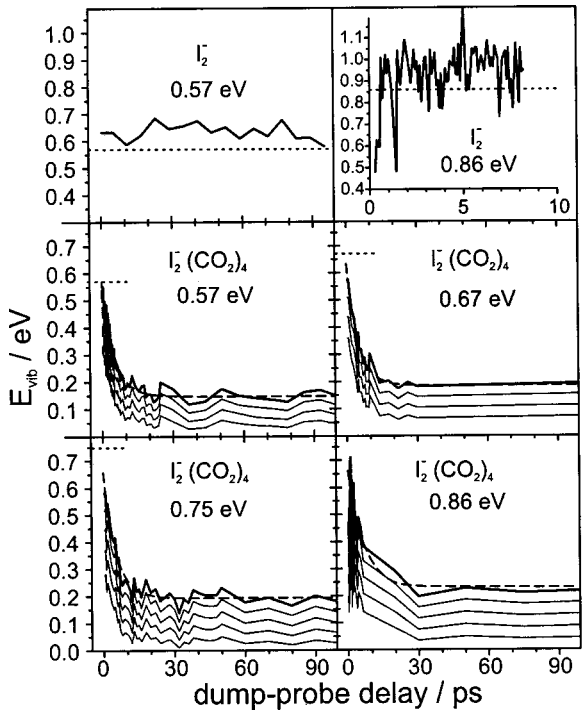

FIG. 8. $E_{vib}(t)$ for bare (top row) and clustered I_2^-, determined from the shift of the spectrum edge. Lines are as described in the caption for Fig. 7.

V. DISCUSSION

The SEP/FPES experiments on $I_2^-(CO_2)_4$ yield two sets of results that enable one to track the relaxation dynamics of vibrationally excited I_2^- within the cluster. During the first 3–4 ps after the pump and dump pulses are applied, we can use oscillations in the time-dependent photoelectron signal at high eKE to monitor the motion of the coherently excited I_2^- wave packet at its inner turning point. The I_2^- moeity behaves like an underdamped oscillator; the observed increase in oscillation frequency with time is a signature of vibrational energy flow from the I_2^- to the surrounding solvent molecules. Based on the straight lines in Fig. 7, the degree of energy flow that occurs while the wave packet maintains its coherence is substantial, representing a significant fraction of E_{exc}. The relaxation dynamics can be followed on a longer time scale, out to 150–200 ps, through observation of the maximum eKE at which signal occurs. These ''edge shifts'' can be fit by a single exponential decay with a time constant on the order of 5 ps.

In this section, these results for $I_2^-(CO_2)_4$ are considered in the context of previous related experiments in clusters and in solution. We then discuss various aspects of the results in more detail, including the relaxation dynamics at very early times, the apparent discrepancies in $E_{vib}(t)$ determined by the two sets of SEP results, and the possible role of solvent evaporation in the experiments.

TABLE II. Parameters for exponential fit of form $E_{vib}=E_0+Ae^{(-t/\tau)}$ to the $n=4$ curves in Figs. 7 and 8.

E_{exc} (eV)	E_0 (eV)	A (eV)	τ (fs)
0.57	0.147±0.005	0.422±0.007	5000±200
0.67	0.185±0.007	0.45±0.01	4800±280
0.75	0.193±0.006	0.47±0.02	5160±390
0.86	0.23±0.025	0.43±0.04	6700±1600

A. Comparison with previous experiments

Earlier studies of the vibrational relaxation of I_2^- have produced vibrationally excited I_2^- in two ways: as a product in the photodissociation of I_3^- in polar solvents, and through photodissociation and subsequent solvent-induced caging of I_2^- in solution and in gas-phase clusters. In solution, vibrational energy flow from the I_2^- produced in both ways was followed by transient absorption[12–15,18,19,21,22] and, for I_3^- photodissociation, by transient response resonance impulsive stimulated Raman scattering (TRISRS).[20,36] In the time-resolved cluster studies by Lineberger and co-workers,[4–6] the overall I_2^- recombination and relaxation time was followed by monitoring recovery of the original absorption at either 720 or 790 nm. This work was complemented by our FPES studies[8,10,11] of $I_2^-(CO_2)_n$ and $I_2^-(Ar)_n$ in which changes in the photoelectron spectrum enabled us to follow dissociation, vibrational relaxation, and solvent evaporation, and by molecular dynamics simulations by Parson,[37–40] Coker,[41–42] and co-workers.

The observation of coherent wavepacket motion provides the first point of comparison between our experiments and the earlier work on I_2^-. No vibrational coherence effects were observed in either the solution or cluster experiments in which I_2^- was formed by solvent-induced caging, presumably because of the substantial interactions between the photofragments and solvent required before recombination can occur. However, the transient absorption experiments of I_3^- photodissociation in ethanol by Ruhman[19] and Vohinger[21] showed oscillations associated with coherent I_2^- vibrational motion for up to 2 ps after the I_3^- photolysis pulse. More recent I_3^- transient absorption data by Hess *et al.*[36] showed the oscillation frequency increasing over this interval. The TRISRS experiments[20,36] performed by both groups induce vibrational coherences which probe the I_2^- vibrational distribution out to 10–15 ps and also show an increase in the I_2^- vibrational frequency with time.

The observed increase in the I_2^- oscillation frequency seen in our SEP experiments is similar to the effect seen in I_3^- photodissociation by Hess *et al.*,[36] and to the ''chirped wave packet dynamics'' seen for the HgBr photoproducts from $HgBr_2$ photodissociation in solution.[43] The frequency shift was not interpreted in terms of vibrational relaxation of the chromophore in either of these studies. In the $HgBr_2$ experiments, it was attributed to rearrangement of the solvent molecules around the photoproducts subsequent to photodissociation, and in the I_3^- experiments to interactions between the separating photofragments. We are in no position to comment on whether either interpretation is correct in the solution-phase experiments, but neither is likely to apply to our experiment because the I_2^- is vibrationally excited by SEP rather than by parent molecule photodissociation.

We can also compare the characteristic relaxation time of 5 ps obtained in our experiment to time constants extracted from previous cluster and solution studies. The $I_2^-(CO_2)_n$ cluster studies by Lineberger and co-workers[4–6]

and the FPES experiments performed in this laboratory[9,11] showed that the overall relaxation times for the I_2^- dropped with increasing solvation. Lineberger[6] found time constants for absorption recovery following photodissociation of $I_2^-(CO_2)_n$ clusters at 790 nm ranging from 24 ps for $n=6$ to 1.3 ps for $n=16$, the latter corresponding to a full solvation shell. Similar time constants for I_2^- formation and relaxation were found in our FPES studies of these clusters.[11] While the amount of caged I_2^- product from $I_2^-(CO_2)_4$ in these experiments was too small to enable its time-dependence to be followed, one would certainly expect even slower relaxation dynamics than in $I_2^-(CO_2)_6$, in seeming contradiction to our relaxation time constants of 5–6 ps. However, the earlier experiments differ from the current work in that the total excitation energy was considerably higher (1.57 eV at 790 nm), the vibrationally excited I_2^- was formed by solvent-induced caging of recoiling photofragments, and I_2^- thus formed initially had more energy (~1 eV). The relatively small variation of the relaxation time constant with excitation energy in our experiment suggests that the last effect is relatively unimportant, so comparison between the SEP results and earlier experiments implies that in the photodissociation experiments on small clusters ($n=4-6$), it takes 10–20 ps for the photofragments to recombine. This interpretation is consistent with our analysis of the $I_2^-(CO_2)_6$ FPE spectrum in which no I_2^- was observed until about 10 ps after the pump (photodissociation) pulse, and highlights the value of performing experiments in which vibrational relaxation can be cleanly separated from caging/recombination dynamics.

Our relaxation times are comparable with those seen for I_2^- solution, a remarkable result in light of the small size of the cluster. A time scale of around 4 ps was seen for vibrational relaxation of I_2^- formed with about 0.2 eV vibrational energy through photodissociation of I_3^- in ethanol.[17,18,44] The experiments by Barbara and co-workers[14] show that starting around 0.3 eV, relaxation takes place with time constants between 3 and 6 ps, with less polar solvents typically exhibiting slower relaxation. However, in Barbara's experiments, the I_2^- is formed by recombination and therefore initially has ~1 eV of vibrational energy. Barbara's interpretation of the transient absorption data is that the I_2^- formed in this manner loses at least half of its ground state vibrational energy within 300 fs.[12–15] This rapid energy loss near the top of the I_2^- well is discussed further in the following sections in the context of the SEP results.

B. Short-time relaxation dynamics

Figure 6 shows that if the linear fits to the frequency shifts in $I_2^-(CO_2)_4$ are extrapolated to $t=0$, the frequencies are considerably higher than those seen when bare I_2^- is excited at the same excitation energy. As a consequence, as shown in Fig. 7, the extrapolated value of E_{vib} at $t=0$ for the cluster is considerably lower than the excitation energy and is approximately independent of E_{exc}, about 0.46 eV for excitations known to be 0.57 eV, 0.67 eV, and 0.75 eV. Moreover, the linear fits to the cluster time-dependent frequencies at 0.57 and 0.67 eV differ by only ~2 cm^{-1} from 0 to 3 ps, whereas the (constant) frequencies for bare I_2^- at these two excitation energies differ by 9 cm^{-1}.

There are two possible contributions to these apparent discrepancies. First, in extracting $E_{vib}(t)$ from the oscillation frequencies, we have assumed the potentials for bare and clustered I_2^- to be the same. This is clearly an approximation; resonant impulsive stimulated Raman scattering results[45] from this laboratory showed a blueshift in the fundamental vibrational frequency in $I_2^-(CO_2)_4$ of 2 cm^{-1} relative to bare I_2^-. As a result, for the same amount of vibrational energy, adjacent energy levels will be further apart in $I_2^-(CO_2)_4$ than in I_2^-, so for the same value of E_{exc} the oscillation frequency would be higher in the cluster. This effect is in the right direction for explaining the difference between bare I_2^- and the extrapolated $t=0$ results for $I_2^-(CO_2)_4$. However, in order for this difference to be *solely* due to the potential being modified by the solvent, the cluster potential would have to be nearly harmonic from 0.57 to 0.75 eV, based on the extrapolated frequencies being nearly identical at $t=0$. But if the potential were harmonic, then as the I_2^- loses energy the wave packet oscillation frequency should not increase with time, in contrast to our observations. Therefore, the potential is not harmonic in this energy range, and the frequency blueshift between bare and clustered I_2^- cannot account for the entire discrepancy between extrapolated and known energies at $t=0$.

A second and probably more important contribution is the occurrence of rapid energy loss from clustered I_2^- that is not measured well by the methods used here. The maxima in the oscillations in Fig. 3 and the high eKE edge shifts in Fig. 4 are sensitive to the inner turning point of the I_2^- vibrational wave function. The first maximum in the oscillations occurs 300–400 fs after the dump pulse, reflecting the fact (see Fig. 1) that the excited state wave packet, once stimulated downward by the dump pulse, continues toward the outer turning point on the ground state potential before reaching the inner turning point for the first time. The magnitude of the energy loss to be accounted for is $\Delta E = E_{exc} - E_{vib}(t_1)$, where t_1 is the time at which the first maximum occurs. If $E_{vib}(t_1)$ is taken from the straight lines in Fig. 7, i.e., assuming the conversion from oscillation frequency to vibrational energy for bare I_2^-, we find ΔE is 140 meV at $E_{exc}=0.57$ eV, 220 meV at 0.67 eV, and 300 meV at 0.75 eV. Since we expect the I_2^- frequencies to be blueshifted in the cluster, these losses represent the maximum amount of energy that has been distributed into the solvent network during the initial wave packet motion. This early time energy loss must be much faster than the subsequent *observed* losses, since linear extrapolation back to $t=0$ does not accurately predict the known initial energy.

There are two opportunities for the I_2^- to lose energy such that we would not easily detect it. The first is on the upper state, in the interval between pump and dump pulses. We have found the optimal pump-dump delay to be between 50 and 190 fs, with longer delay times generally working better for higher excitation energies. The longer the wave-packet remains on the upper state before being transferred to the ground state via SEP, the more opportunity there is for

energy transfer on the upper state from the recoiling fragments to the solvent molecules. However, the recombination yield for $I_2^-(CO_2)_4$ at 790 nm is only 3%,[46] indicating a weak interaction between the recoiling fragments and solvent molecules. Our FPES experiments on $I_2^-(CO_2)_4$ indicate that some solvent dynamics do occur, but only after 300 fs, i.e., after the I_2^- bond has broken.[11,31] We thus regard it as unlikely that upper state energy loss prior to application of the dump pulse is primarily responsible for the effects under consideration.

Energy loss more likely occurs on the ground state, between the dump pulse and the first arrival of the wave packet at the inner turning point. The I_2^- charge distribution should become highly localized as the outer turning point is approached at the high excitation energies used in our experiment, with most of the excess charge localized on one I atom. In the next phase of the wave packet motion, between the first outer and inner turning point encounters, the charge distribution rapidly switches back to a delocalized distribution with comparable charge on both I atoms. Simulations in $I_2^-(CO_2)_n$ clusters by Papanikolas *et al.*[39] and I_2^- in solution by Benjamin *et al.*[47] show that this change in the electronic character of the I_2^- results in strong coupling with the solvent molecules and leads to rapid energy transfer from the I_2^- to the surrounding solvent. While these dynamics are operative throughout the entire relaxation process, the simulations indicate the most effective energy transfer accompanies the largest excursions in the I_2 bond length. This rapid energy loss high in the potential well agrees with conclusions drawn from previous experimental work on I_2^- relaxation in solution, in particular the finding in polar solvents[13–15] that I_2^- photodissociated at 780 nm recombines and loses ~0.7 eV of its vibrational energy in the extremely short time of 300 fs.

The occurrence of rapid energy loss at early times is also supported by the $E_{vib}(t)$ values in Fig. 7 extracted from the high eKE edge positions. If the exponential fits to these results are extrapolated to $t=0$ (see Table II), we find that $E_{vib}(0)=0.57$ eV at $E_{exc}=0.57$ eV, $E_{vib}(0)=0.63$ eV at $E_{exc}=0.67$ eV, $E_{vib}(0)=0.66$ eV at $E_{exc}=0.75$ eV, and $E_{vib}(0)=0.67$ eV at $E_{exc}=0.86$ eV. As noted in Sec. IV the energy calculated from the edge position overestimates $E_{vib}(t)$, so if these values of $E_{vib}(0)$ were correct, they should be larger than the known initial vibrational energy E_{exc}. The observation that extrapolation at best matches E_{exc} (at $E_{exc}=0.57$ eV) or underestimates it (all higher E_{exc}) implies rapid energy loss at very early times that cannot be fit by the exponential function describing relaxation after 300–400 fs.

C. Longer-time dynamics

Figure 7 shows that at dump-probe delays ranging from 300 fs to 3–4 ps, we can directly examine and compare the I_2^- vibrational energies $E_{vib}(t)$ derived from the time-dependent frequencies and the shift of the spectra. At the three lowest excitation energies, $E_{vib}(t)$ derived from the edge shifts consistently lies above $E_{vib}(t)$ derived from the time-dependent frequencies. As discussed above, the edge shifts overestimate $E_{vib}(t)$, whereas $E_{vib}(t)$ is underestimated when determined by the frequency shifts because the vibrational frequency of clustered I_2^- is blueshifted compared that of bare I_2^-.[45] Hence, the conservative interpretation of Fig. 7 is that the true value of $E_{vib}(t)$ is bracketed by the two methods. At 0.57 and 0.67 eV, the values of $E_{vib}(t)$ determined from the frequencies decrease more rapidly than those determined by the edge shifts. This difference could result from the assumed linear fit to the frequency shifts. In addition, the evaporation of a solvent molecule would shift the edge energies onto the lower ($n=3$) curve, and could help explain the difference in rates of observed energy loss. Such a process would be energetically possible within the first 2 ps for the lower two excitations given the amount of energy lost to the solvent molecules, based on the binding energy of the fourth CO_2 (175 meV) determined in our photofragment mass spectrometry studies.[30] Our FPE spectra of $I_2^-(CO_2)_n$ clusters indicated that some solvent evaporation takes place on this time scale, but in those experiments the recoiling photofragments transfer a significant amount of energy to the solvent within 1 ps of excitation, so the earlier results may not be comparable to the gentler excitation scheme used in the SEP experiment.

While the energies derived from frequency and edge position diverge with time for the two lowest SEP excitations, at $E_{exc}=0.75$ eV the situation is reversed: the edge shift analysis shows energy being lost *more* quickly than the frequency analysis, so that by the end of the oscillations, 2900 fs, E_{vib} is bracketed between 0.40 eV (from the frequency) and 0.46 eV (from the fit to the edge data, assuming no evaporation). The significance of the small frequency increase at 0.75 eV excitation is difficult to determine. We speculate that it is related to the overall shape of the oscillations at the inner turning point (see Fig. 3); the average intensity underlying the oscillations at the inner turning point does not peak until the 3rd or 4th oscillation, which implies that much of the SEP intensity does *not* oscillate, but rather arrives monotonically at the inner turning point around 1.5 ps. Additionally, the oscillation depth is quite small compared to the average intensity at this excitation. The oscillations at 0.86 eV are even more tenuous. It seems that only a minor portion of the wave packet excited with 0.75 or 0.86 eV oscillates, and that at these energies, the oscillation frequency may not be a good measure of the average vibrational excitation. One issue to consider at these two higher energies is that at the outer turning point, where the excess charge should be largely localized on a single I atom, the interaction between the charged atom with the CO_2 molecules is comparable or stronger than that between the two I atoms, keeping in mind that the $I^-(CO_2)$ bond dissociation energy is 0.21 eV.[48] This effect may perturb the wave packet dynamics sufficiently to introduce a significant nonoscillatory component.

At longer times, after the oscillations have disappeared, the only measure of energy loss comes from the shift of the high eKE edge of the spectra. We can examine and compare the exponential fits to the energy derived assuming four solvent molecules (Fig. 8). We have already discussed the initial ($t=0$) energy, and the decay time constants are more or less the same for all energies except 0.86 eV (which has a large

error bar associated with it). This leaves the asymptotic energy E_0, which increases only slightly with E_{exc} (see Table II). The significance of this parameter depends on whether CO_2 evaporation occurs over the time scale of the measurement. If no evaporation occurs, E_0 represents energy that remains as I_2^- vibration, and in a small cluster like $I_2^-(CO_2)_4$, one can understand E_0 remaining positive at long times in terms of equilibration of energy between the I_2^- and low frequency solvent vibrational modes. In fact, for all four excitation energies, the ratio E_0/E_{exc} is between 0.25 and 0.27, i.e., essentially a constant, which would be consistent with this interpretation of E_0. On the other hand, as discussed in Sec. IV, when a CO_2 molecule evaporates, the difference between anion and neutral potentials decreases, and so a given vibrational energy assuming n CO_2 molecules corresponds to a smaller vibrational energy assuming $n-1$ molecules remain. Thus, E_0 represents an upper bound to the true value of $E_{vib}(t)$, with the difference between the apparent and true values depending on how much evaporation has occurred by time t.

In our previous analysis of the FPE spectra of $I_2^-(CO_2)_n$ clusters,[11] it was possible to separate vibrational relaxation from solvent evaporation by examining the energy range of the PE spectrum corresponding to the *outer* turning point of the vibrationally excited I_2^-. This analysis was not entirely unambiguous, but it did imply that there was a significant time delay between vibrational relaxation and solvent evaporation, and this delay is likely to occur in the SEP experiments as well. Ideally, a similar analysis could be applied to the SEP-induced photoelectron spectra measured here to determine the actual number of solvent molecules remaining at a given time, but in practice the outer turning point eKE range is too influenced by depletion due to the dump pulse, an additional complication not present in the pump–probe FPES study, to extract solvent numbers with much confidence. The question of the time scale for evaporation thus remains somewhat of an open question, one that certainly could be addressed in molecular dynamics simulations.

VI. CONCLUSIONS

In this paper, we have shown that femtosecond stimulated emission pumping can be used to excite the I_2^- chromophore in $I_2^-(CO_2)_4$ and produce a coherent superposition of vibrational levels with a well-defined and easily adjustable average vibrational energy. The time-evolution of this wave packet can then be followed using femtosecond photoelectron spectroscopy. The pump-dump-probe scheme used to effect this was previously applied to bare I_2^-; here we use it to follow the dynamics of energy flow from the vibrationally excited I_2^- to the surrounding solvent molecules.

The experiment yields two observables associated with the inner turning point of the wavepacket that essentially allow one to follow vibrational relaxation in real time. First, at high electron kinetic energy, we observe oscillations for several ps after the dump pulse associated with wave packet recurrences at the inner turning point. The frequency of these oscillations increases with time, signifying vibrational relaxation in an anharmonic potential where the spacing between adjacent vibrational levels increases as the I_2^- drops lower in the well. In addition, the maximum electron kinetic energy at which signal is observed provides a measure of the I_2^- vibrational energy at longer times, out to 100–200 ps. The key results obtained from this work are (a) the I_2^- loses 0.2–0.4 eV of vibrational energy in the first few ps while maintaining its coherence, and (b) vibrational relaxation after 300 fs can be fit by a single exponential decay with a time constant of about 5 ps, comparable to that seen for I_2^- with a similar amount of vibrational energy in solution.

Detailed analysis of the results reveals two issues regarding the overall dynamics that require further characterization. Extrapolation of both the frequency shifts and the high electron energy edge shifts to zero time indicates that there is very rapid vibrational energy loss within the first 300 fs after the dump pulse. This situation is reminiscent of results in solution where I_2^- formed by recombination loses 0.6–0.7 eV of vibrational energy within the first 300 fs before exhibiting exponential decay with a much longer time constant. In addition, by 2 ps, enough energy has been transferred to the solvent molecules for evaporation to occur, but the extent to which this happens cannot be ascertained from our experiment.

Future experimental work in our laboratory will focus on how the effects seen here vary with the number and type of solvent species. Results for larger $I_2^-(CO_2)_n$ clusters and a series of $I_2^-(Ar)_n$ clusters have been obtained and are currently being analyzed. It would clearly be of interest to apply our femtosecond SEP scheme to I_2^- in solution and use transient absorption to monitor the ensuing dynamics; such an experiment (which we do not plan to perform ourselves) would provide a detailed comparison between vibrational relaxation in clusters and in solution. In addition, the interpretation of the results presented here would be enhanced significantly by means of the classical molecular dynamics simulations that were so useful in interpreting earlier work on clustered I_2^-, and by more sophisticated quantum mechanical simulations which could provide important insights into the damped coherent motion that features so prominently in our results.

ACKNOWLEDGMENTS

This research is supported by the National Science Foundation under Grant No. CHE-0092574. A.E.B. is a NSF predoctoral fellow. R.W. acknowledges support from the Alexander von Humboldt-Stiftung and from the Emmy Noether-Programm of the Deutsche Forschungsgemeinschaft.

[1] G. W. Flynn, C. S. Parmenter, and A. M. Wodtke, J. Phys. Chem. **100**, 12817 (1996).
[2] M. Silva, R. Jongma, R. W. Field, and A. M. Wodtke, Annu. Rev. Phys. Chem. **52**, 811 (2001).
[3] R. M. Stratt and M. Maroncelli, J. Phys. Chem. **100**, 12981 (1996).
[4] J. M. Papanikolas, J. R. Gord, N. E. Levinger, D. Ray, V. Vorsa, and W. C. Lineberger, J. Phys. Chem. **95**, 8028 (1991).
[5] J. M. Papanikolas, V. Vorsa, M. E. Nadal, P. J. Campagnola, H. K. Buchenau, and W. C. Lineberger, J. Chem. Phys. **99**, 8733 (1993).
[6] V. Vorsa, S. Nandi, P. J. Campagnola, M. Larsson, and W. C. Lineberger, J. Chem. Phys. **106**, 1402 (1997).
[7] A. Sanov, T. Sanford, S. Nandi, and W. C. Lineberger, J. Chem. Phys. **111**, 664 (1999).

[8] B. J. Greenblatt, M. T. Zanni, and D. M. Neumark, Science **276**, 1675 (1997).
[9] B. J. Greenblatt, M. T. Zanni, and D. M. Neumark, Faraday Discuss. **108**, 101 (1998).
[10] B. J. Greenblatt, M. T. Zanni, and D. M. Neumark, J. Chem. Phys. **111**, 10566 (1999).
[11] B. J. Greenblatt, M. T. Zanni, and D. M. Neumark, J. Chem. Phys. **112**, 601 (2000).
[12] A. E. Johnson, N. E. Levinger, and P. F. Barbara, J. Phys. Chem. **96**, 7841 (1992).
[13] D. A. V. Kliner, J. C. Alfano, and P. F. Barbara, J. Chem. Phys. **98**, 5375 (1993).
[14] P. K. Walhout, J. C. Alfano, K. A. M. Thakur, and P. F. Barbara, J. Phys. Chem. **99**, 7568 (1995).
[15] J. C. Alfano, Y. Kimura, P. K. Walhout, and P. F. Barbara, Chem. Phys. **175**, 147 (1993).
[16] E. Gershgoren, U. Banin, and S. Ruhman, J. Phys. Chem. A **102**, 9 (1998).
[17] U. Banin and S. Ruhman, J. Chem. Phys. **99**, 9318 (1993).
[18] U. Banin, A. Waldman, and S. Ruhman, J. Chem. Phys. **96**, 2416 (1992).
[19] U. Banin and S. Ruhman, J. Chem. Phys. **98**, 4391 (1993).
[20] U. Banin, R. Kosloff, and S. Ruhman, Chem. Phys. **183**, 289 (1994).
[21] T. Kühne and P. Vöhringer, J. Chem. Phys. **105**, 10788 (1996).
[22] T. Kühne, R. Küster, and P. Vöhringer, Chem. Phys. **233**, 161 (1998).
[23] R. Pausch, M. Heid, T. Chen, W. Kiefer, and H. Schwoerer, J. Chem. Phys. **110**, 9560 (1999).
[24] G. Knopp, I. Pinkas, and Y. Prior, J. Raman Spectrosc. **31**, 51 (2000).
[25] M. T. Zanni, A. V. Davis, C. Frischkorn, M. Elhanine, and D. M. Neumark, J. Chem. Phys. **113**, 8854 (2000).
[26] A. Materny, T. Chen, M. Schmitt, T. Siebert, A. Vierheilig, V. Engel, and W. Kiefer, Appl. Phys. B: Lasers Opt. **B71**, 299 (2000).
[27] I. Pinkas, G. Knopp, and Y. Prior, J. Chem. Phys. **115**, 236 (2001).
[28] D. M. Neumark, Annu. Rev. Phys. Chem. **52**, 255 (2001).
[29] A. V. Davis, M. T. Zanni, C. Frischkorn, M. Elhanine, and D. M. Neumark, J. Electron Spectrosc. Relat. Phenom. **112**, 221 (2000).
[30] R. Wester, A. V. Davis, A. E. Bragg, and D. M. Neumark, Phys. Rev. A **65**, 051201 (2002).
[31] M. T. Zanni, V. S. Batista, B. J. Greenblatt, W. H. Miller, and D. M. Neumark, J. Chem. Phys. **110**, 3748 (1998).
[32] H. Gómez, T. R. Taylor, and D. M. Neumark, J. Chem. Phys. **116**, 6111 (2002).
[33] R. J. LeRoy, J. Chem. Phys. **52**, 2683 (1970).
[34] S. Gerstenkorn and P. Luc, J. Phys. (Paris) **46**, 867 (1985).
[35] F. Martin, R. Bacis, S. Churassy, and J. Verges, J. Mol. Spectrosc. **116**, 71 (1986).
[36] S. Hess, H. Bürsing, and P. Vöhringer, J. Chem. Phys. **111**, 5461 (1999).
[37] J. Faeder, N. Delaney, P. E. Maslen, and R. Parson, Chem. Phys. Lett. **270**, 196 (1997).
[38] J. Faeder, N. Delaney, P. E. Maslen, and R. Parson, Chem. Phys. **239**, 525 (1998).
[39] J. M. Papanikolas, P. E. Maslen, and R. Parson, J. Chem. Phys. **102**, 2452 (1995).
[40] R. Parson, J. Faeder, and N. Delaney, J. Phys. Chem. A **104**, 9653 (2000).
[41] V. S. Batista and D. F. Coker, J. Chem. Phys. **106**, 7102 (1997).
[42] C. J. Margulis and D. F. Coker, J. Chem. Phys. **110**, 5677 (1999).
[43] M. Lim, M. F. Wolford, P. Hamm, and R. H. Hochstrasser, Chem. Phys. Lett. **290**, 355 (1998).
[44] I. Benjamin, U. Banin, and S. Ruhman, J. Chem. Phys. **98**, 8337 (1993).
[45] M. T. Zanni, B. J. Greenblatt, and D. M. Neumark, J. Chem. Phys. **109**, 9648 (1998).
[46] V. Vorsa, Ph.D. thesis, University of Colorado, Boulder, 1996.
[47] I. Benjamin, P. F. Barbara, B. J. Gertner, and J. T. Hynes, J. Phys. Chem. **99**, 7557 (1995).
[48] Y. X. Zhao, C. C. Arnold, and D. M. Neumark, J. Chem. Soc., Faraday Trans. **89**, 1449 (1993).
[49] N. Delaney, J. Faeder, and R. Parson (private communication).